Applied Radiation and Isotopes xxx (xxxx) 110238

Contents lists available at ScienceDirect

Applied Radiation and Isotopes

journal homepage: www.elsevier.com/locate/apradiso

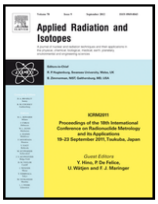

# Separation of radium and actinium using zirconia

M. Alex Brown

*Chemical & Fuel Cycle Technologies Division, Argonne National Laboratory, 9700 S. Cass Ave, Lemont, IL, 60439, USA*

ARTICLE INFO

*Keywords:*
*Radium*
*Actinium*
*Lead*
*Zirconia*
*Radiochemistry*
*Separations*
*Medical isotopes*
*Alpha therapy*

ABSTRACT

Zirconia was investigated as a radiation-resistant support for radium and actinium aqueous ion separations. Acetate and total metal ion concentrations were experimentally evaluated as factors that could affect retention using La and Ba surrogates. Pseudo-second order rate constants were derived and the uptake of La was determined to be endothermic. Elution profiles containing Ba, La, $^{228}$Ra, $^{228}$Ac, and $^{212}$Pb are presented and discussed.

## 1. Introduction

The demand for alpha-emitting isotopes with relatively short half-lives is increasing for use in radionuclide therapy (Eychenne et al., 2021). Remarkable results are achievable by leveraging the cytotoxic doses that alpha particles can deliver to malignant tissues when the isotope is properly chelated and conjugated to a targeting vector. (Dadachova and Casadevall, 2009), (Kratochwil et al., 2016) In 2013, the U.S. FDA approved the use of $^{223}$Ra ($t_{½}$ = 11.4 d) and in recent years $^{225}$Ac ($t_{½}$ = 9.9 d) has emerged as a promising, high-priority candidate. The isotopes can be produced in large quantities using accelerators, reactors, or aged actinide stocks and purifications are commonly executed using ion-exchange or extraction chromatography. (Ferrier et al., 2019), (Radchenko et al., 2021), (Nagatsu et al., 2021) Consequently, extreme doses ($>10^8$ cGy) in solution are to be expected during the initial processing of these activated targets as well as any generators that involve alpha-emitters (Mcdevitt et al., 1999). Given that all organic polymer supports are susceptible to radiolysis, it is not surprising that unusual or even catastrophic results (unreproducible or low yields, resin discoloration, organic impurities, flow resistance or blockage) have been documented while processing large quantities of radium, thorium, actinium, americium, bismuth, or lead isotopes by conventional resins. (Mcdevitt et al., 1999), (Kirby et al., 2006), (Power et al., 1959), (Boll et al., 2005), (Boll et al., 1997)., (Vasiliev et al., 2020)

The focus here is on production channels that use radium targets. To combat the high radiation fields while maintaining effective separation capabilities, inorganic supports can offer some utility and are already applied to medical isotope technologies ($^{99}$Mo/$^{99m}$Tc generators) and nuclear waste management. (Mirzadeh et al., 2003), (Schulz et al., 1980) A recent experimental campaign screened three metal oxide sorbents as potential platforms for the separation of radium and actinium: alumina, titania, and zirconia (Brown, 2020). Judgements based on chemical compatibility with acids and Ba/La surrogate static retention studies led to a more concerted focus on zirconia where excellent separation bands between Ra/Ac tracers were achieved on a stationary 1-g $ZrO_2$ column. The eluates consisted of sodium acetate and HCl. Consistent with many ion-exchange platforms, the most sensitive variable was pH where pH 5–6 and pH 3–4 were determined to be the ideal windows to separate Ba/La and Ra/Ac/Pb, respectively. Below pH 3, the $H^+$ ions competed with the lanthanide or actinide ions and the uptake was suppressed. Above pH 6, the uptake of both divalent and trivalent ions increased which ultimately decreased the selectivity. Consequently, acetate was chosen as the aqueous buffer in view of its buffer capacity ($pK_a$ = 4.7) and relatively weak complexation affinity with trivalent lanthanides and actinides. The purpose of this work was to explore additional variables that could influence and improve decontamination factors: concentrations, kinetics, temperature, and stable carriers.

## 2. Experimental

Zirconia (ZirChrom-PHASE, Sachtopore, monoclinic, 25 µm, 300 Å, surface area: 30 $m^2/g$) was used as received. More information pertaining to this sorbent, including surface chemistry, physical parameters, and x-ray diffractions, can be found in the literature. (Nawrocki et al.,

---

*E-mail address:* brownma@anl.gov.

https://doi.org/10.1016/j.apradiso.2022.110238
Received 25 January 2022; Received in revised form 4 April 2022; Accepted 7 April 2022
0969-8043/© 20XX

1993)’ (Nawrocki et al., 2004) Aqueous solutions contained de-ionized water (18 MΩ cm). Nitric acid solutions were prepared by diluting a concentrated stock (Fisher, trace metal grade). Hydrochloric acid solutions were prepared from a concentrated stock (Fisher, Optima grade). Barium (Fisher ACS, >99%) and lanthanum (Alfa-Aesar ACS, 99.99%) stocks were prepared by dissolving the hydrated nitrate salts. Solutions of acetate were prepared from Ultra-Pure ammonium or sodium acetate (VWR). The pH of equilibrated solutions was measured using an Ag/AgCl combination glass electrode that was calibrated with 1.68, 4.01, and 7.00 NIST standardized buffers.

A stock solution of $^{228}$Ra was prepared from aged $^{232}Th(NO_3)_4$-hydrate (Mallinckrodt). The purification process was described previously (Brown, 2020). In short, the ~50 year-old thorium salt was dissolved in nitric acid and processed via solvent extraction (2 × HDEHP; 2 × TODGA) and extraction chromatography (DGA, Eichrom) then aged for several years to allow in-growth of high specific activity $^{228}$Th ($t_{½}$ = 1.9 y) as well as $^{228}$Ra ($t_{½}$ = 5.7 y), $^{224}$Ra ($t_{½}$ = 3.6 d), $^{228}$Ac ($t_{½}$ = 6.1 h), and $^{212}$Pb ($t_{½}$ = 10.6 h). Analysis was performed using a high-purity germanium detector with GammaVision software (338 keV $^{228}$Ac, 241 keV $^{224}$Ra, 238 keV $^{212}$Pb). Activities were decay corrected to the time of separation with the exception of the 25 h decay measurements. Determination of $^{228}$Ra was performed five days after separations to allow for equilibrium in-growth of the $^{228}$Ac daughter.

Partition coefficients were determined by equilibrating a mixture of Ba and La with a known volume (2–5 mL) of solution and known mass (~100 mg, ~50–100 × excess of the La or Ba ion) of dry sorbent for at least 24 h with periodic agitation. Controlled temperature experiments were performed using a Julaboo shaker/bath with a temperature variation of ±0.1 °C. The La and Ba concentrations varied between $10^{-4}$–$10^{-1}$ M. After equilibration, one portion of the supernatant was decanted, filtered through a 0.45 μm syringe filter, and submitted for inductively coupled plasma – mass spectrometry (ICP-MS). The remaining fraction was used to measure the equilibrium pH of the solutions. Each column trial utilized a fixed mass of zirconia packed with glass wool in an 8 mL, non-jacketed, chromatography column (Millipore Sigma, 1 cm × 10 cm). The columns were washed with 10 mL of $H_2O$ followed by 15 mL of acetate solution with the desired pH. The feed solution comprised a known Ba/La or Ra/Ac/Pb mixture. Various eluates containing sodium acetate or HCl of different pH were explored to develop elution profiles. A slight positive pressure was applied to the column resulting in a flow rate of 2.0 mL/min. Results were determined by ICP-MS or γ-analysis.

## 3. Results & discussion

Partition coefficients ($K_D$) for selected ions were determined in terms of dry sorbent mass ($m$) and a fixed volume ($V$) where $C_0$ and $C$ represent the initial and final concentrations of the ions, respectively. Units are presented in mL/g.

$$K_D = \left(\frac{C_0}{C} - 1\right)\frac{V}{m} \qquad (1)$$

Fig. 1 presents a compilation of static sorption results using stable Ba and La with zirconia. Fig. 1A plots the influence of acetate concentration on the uptake of Ba or La at a fixed pH of 5.55 ± 0.05. A clear relationship between the acetate concentration and La retention was observed; Ba exhibited a relatively consistent minimal sorption throughout which resulted in high uncertainties when analyzed by ICP-MS. The decrease in La uptake was most likely correlated to the complexation chemistry of $La^{3+}$ with deprotonated acetate ligands ($L^-$). The reported stability constants of $La(L)^{2+}$ and $La(L)_2^{+}$ at 1 M ionic strength are $10^{1.53}$ and $10^{2.43}$, respectively (Lopes et al., 2006). For acetate conditions similar to Fig. 1A ($10^{-2} < [L] < 10^{\circ}$), the aqueous speciation of La ranged from initially 77% $La^{3+}$, 22% $La(L)^{2+}$, 1% $La(L)_2^{+}$ to <1% $La^{3+}$, 12% $La(L)^{2+}$, 88% $La(L)_2^{+}$. Presuming that $La^{3+}$ was the targeted species on zirconia the increase in complexed metal ions can explain the decreased ion uptake. From an applied perspective, lower acetate concentrations could increase the separation factors between Ba/La or Ra/Ac while simultaneously minimizing competition from acetate during isotope chelation. It should also be noted that a weak buffer was required to fix pH since the sorbents can exhibit slightly basic tendencies resulting in pH fluctuations in the presence of only a mineral acid (Brown, 2020). Expectedly, in Fig. 1B, the sorption of La decreased with increasing metal ion concentrations as binding sites were populated.

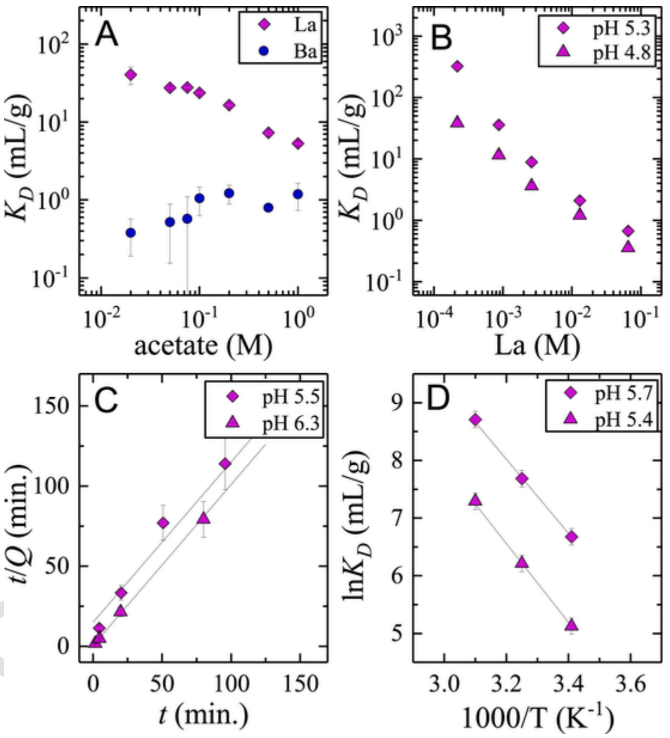

**Fig. 1.** Static partition coefficients of Ba and La with zirconia in solutions of sodium acetate. A): partition coefficients as a function of acetate concentration at a fixed pH of 5.55 ± 0.05 and room temperature (n = 3); $[Ba]_0$ = 1.2 mM, $[La]_0$ = 0.75 mM. B): partition coefficients of La at room temperature as a function of initial La concentration at pH 5.3 ± 0.3 and pH = 4.8 ± 0.2. C): time-dependent sorption of $[La]_0$ = 0.75 mM at room temperature; solid lines represent a slope of 1. D): partition coefficients of La as a function of temperature; $[La]_0$ = 0.07 mM, pH = 5.74 ± 0.01, and pH = 5.41 ± 0.01. Uncertainties plotted in B-D are quantified at ± $K_D$ × 14% or ± Q × 14% based on ICP-MS analysis.

The kinetics and thermodynamics of La sorption on zirconia were evaluated and the results are plotted in Fig. 1C and D. A number of sorption kinetic studies using actinium or actinide ions with inorganic supports determined pseudo-second order kinetic rate constants as opposed to pseudo-first order. (Severin et al., 2020)’ (Karmakar et al., 2020) The sorption extent, $Q$, can be defined in terms of mmol La sorption per gram at time $t$ ($q_t$) and equilibrium ($q_e$): $Q = q_t/q_e$. Pseudo-second order kinetic models incorporate this term:

$$\frac{t}{Q} = \frac{1}{k_2 q_e} + t \qquad (2)$$

The rate constant, $k_2$ (g/mmol/min.), can be determined from a plot of $t/Q$ vs. $t$ provided that a unit slope is observed. Two sets of zirconia sorption studies at a fixed pH of 5.5 and 6.3 were evaluated against time and are plotted in Fig. 1C. From the intercepts of the trend lines, the rate constants were determined to be 1.4 × $10^2$ g/mmol/min ($R^2$ = 0.98) and 1.2 × $10^1$ g/mmol/min ($R^2$ = 0.99) for pH 6.3 and 5.5, respectively, indicating more rapid sorption at the lower acidity.

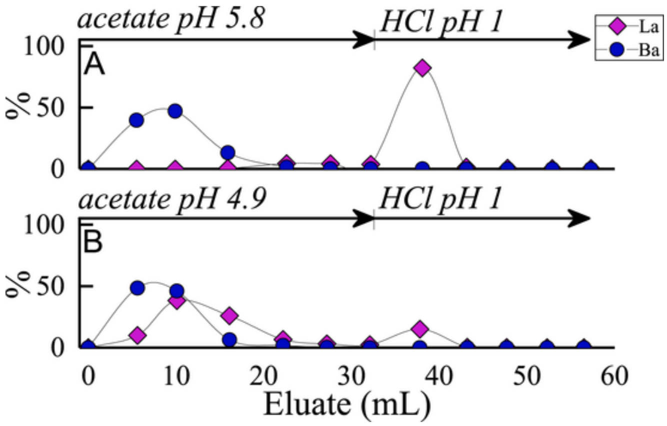

**Fig. 2.** Elution of La ($[La]_0$ = 0.4 mM) and Ba ($[Ba]_0$ = 0.7 mM) from zirconia at room temperature using 75 mM acetate and HCl. A: 75 mM acetate (pH 5.8); B: 75 mM acetate (pH 4.9). The resin mass = 0.5 g, column diameter = 1 cm, flow rate of 2.0 mL/min at room temperature. The elution curves serve as a visual aid.

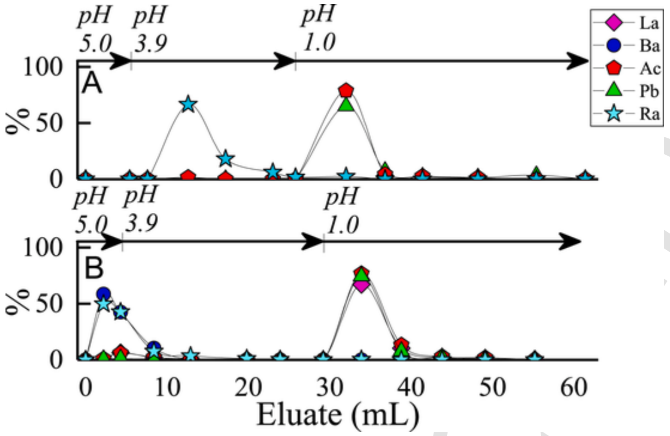

**Fig. 3.** (A) Elution of tracer quantities of $^{212}$Pb, $^{228}$Ra, and $^{228}$Ac using 75 mM acetate (pH 5.0, pH 3.9) and HCl (pH 1.0). (B) Elution of tracer quantities of $^{212}$Pb, $^{228}$Ra, $^{228}$Ac, with stable Ba ($[Ba]_0$ = 0.8 mM), and La ($[La]_0$ = 0.01 mM) using 75 mM acetate (pH 5.0, pH 3.9) and HCl (pH 1.0). The resin mass = 1.0 g, column diameter = 1 cm, flow rate = 2.0 mL/min at room temperature. The elution curves serve as a visual aid.

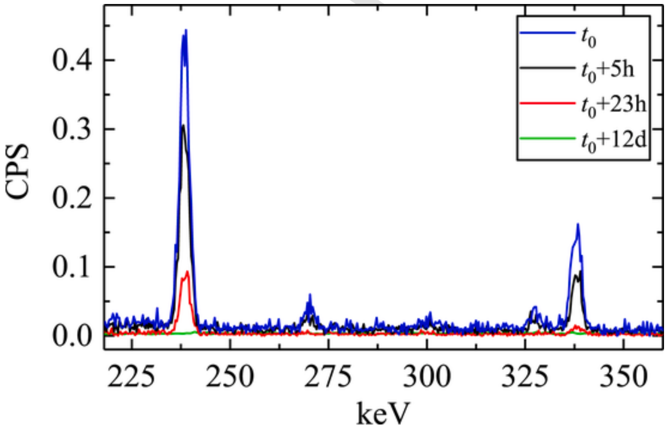

**Fig. 4.** Time-dependent, γ-spectra in counts per second (CPS) of the pH 1.0 product described in Fig. 3(B) showing purified $^{228}$Ac (338 keV) and $^{212}$Pb (238 keV).

The sorption of La increased with temperature as plotted in Fig. 1D. At a fixed pH of 5.7, raising the temperature from 20 °C to 50 °C increased the $K_D$ by a factor of 7.6. With constant ionic strength and in the presence of excess sorbent relative to the metal ion, the semi-log Van't Hoff relationship can be used to determine enthalpies and entropies. (Karmakar et al., 2020)' (Talip et al., 2009) The values of $\ln K_D$ decreased linearly with inverse temperature ($R^2$ = 0.99) and from the slopes and intercepts of each trend, the average enthalpy and entropy were determined to be 55 ± 2 kJ/mol and 236 ± 1 J/mol/K, respectively. The uptake of La by zirconia was endothermic with a positive entropy contribution that contributed to the overall stability of the reaction. This is generally consistent with the entropy gain associated with the complexation and dehydration of a lanthanide or actinide ion (Choppin, 1983).

Of the parameters described above to improve Ra/Ac decontamination factors, the most convenient to leverage was the acetate concentration. Fig. 2 plots the elution profiles of Ba/La using 75 mM acetate and HCl at various pH. With pH 5.8 acetate, the separation bands were very well resolved and are similar to the results obtained previously with the added benefit of less acetate present (Brown, 2020). The decontamination factor, defined here as ratio of initial $[Ba]_i/[La]_i$ and final $[Ba]_f/[La]_f$ was equal to 469. The elution bands using pH 4.9 were not resolved in accordance with the high pH sensitivity that the zirconia platform exhibits.

Fig. 3A plots the elution profile of Ra, Ac, and Pb using 75 mM acetate or HCl at various pH and 1.0-g of zirconia. The pH 5.0 acetate loaded all three isotopes onto the column while the pH 3.9 acetate wash removed radium in approximately 20 mL. The HCl wash removed the remaining actinium and lead along with roughly 2% radium carryover which indicates more acetate could have probably improved the separation.

The column experiment was repeated in the presence of stable Ba and La and the results are plotted in Fig. 3B. In contrast to the results in Fig. 3A, the majority of the Ra and Ba were eluted during the acetate (pH 5.0) loading step while the subsequent acetate (pH 3.9) removed the remainder. These results support the notion that the stable Ba (0.8 mM) carried the trace Ra which altered the elution band. Additionally, an anonymous reviewer pointed out that local saturation could potentially play a role. Local saturation by the macro components (Ba + La) on the column bed has the potential to shift the elution profile of the tracer to the left. When the exchange sites become populated the tracer travels a further distance along the column. This trend was reported in the case of trace and macro-quantities of Ca, Ba, and La on $NH_4^+$ exchange platforms (Massart, 1971). The La and Ac were unaffected and the relative quantities were nearly identical in the HCl washes along with the majority of Pb. The decontamination factor, defined as the ratio of $[Ra]_i/[Ac]_i$ and $[Ra]_f/[Ac]_f$, was 284 and the recovery of Ac was determined to be 94% with a 0.3% Ra impurity in the product. The first 5 mL fraction of the HCl product containing the majority of the $^{228}$Ac and $^{212}$Pb isotopes was analyzed over an extended period of time. Each isotope exhibited a consistent decay close to their respective half-lives down to near-background levels after one week. The γ-spectra are plotted in Fig. 4.

The results further support the applicability of radiation-resistant metal oxide sorbents like zirconia for the separation of radium and actinium. More work is needed to verify and validate that these sorbents can in fact be used in the presence of high-radiation fields. It is also important to understand the elution behavior of notable impurities generated from side reactions, decay chains, or natural impurities including isotopes of Bi, Po, and Th.

## CRediT authorship contribution statement

**M. Alex Brown:** Writing – review & editing, Writing – original draft, Visualization, Validation, Supervision, Software, Resources, Project administration, Methodology, Investigation, Funding acquisition, Formal analysis, Data curation, Conceptualization.

## Declaration of competing interest

The authors declare that they have no known competing financial interests or personal relationships that could have appeared to influence the work reported in this paper.

## Acknowledgments

This research is supported by the U.S. Department of Energy Isotope Program, managed by the Office of Science for Isotope R&D and Production. Argonne National Laboratory and the Office of Science is part of the U.S. Department of Energy contract DEAC02-06CH11357. The U.S. Government retains for itself, and others acting on its behalf, a paid-up nonexclusive, irrevocable worldwide license in said article to reproduce, prepare derivative works, distribute copies to the public, and perform publicly and display publicly, by or on behalf of the Government. The author would like to thank Yifen Tsai of the Argonne Analytical Chemistry Laboratory for ICP-MS analysis and discussion.

## References

Boll, R.A., Mirzadeh, S., Kennel, S.J., 1997. Optimizations of radiolabeling of immunoproteins with Bi-213. Radiochim. Acta 79, 145–149.

Boll, R.A., Malkemus, D., Mirzadeh, S., 2005. Production of actinium-225 for alpha particle mediated radioimmunotherapy. Appl. Radiat. Isot. 62 (5), 667–679.

Brown, M.A., 2020. Metal oxide sorbents for the separation of radium and actinium. Ind. Eng. Chem. Res. 59 (46), 20472–20477.

Choppin, G.R., 1983. Comparison of the solution chemistry of the actinides and lanthanides. J. Less Common. Met. 93, 323–330.

Dadachova, E., Casadevall, A., 2009. Radioimmunotherapy of infectious diseases. Semin. Nucl. Med. 39 (2), 146–153.

Eychenne, R., Cherel, M., Haddad, F., Guerard, F., Gestin, J.F., 2021. Overview of the most promising radionuclides for targeted alpha therapy: the "Hopeful Eight. Pharmaceutics 13 (6).

Ferrier, M.G., Radchenko, V., Wilbur, D.S., 2019. Radiochemical aspects of alpha emitting radionuclides for medical application. Radiochim. Acta 107 (9–11), 1065–1085.

Karmakar, R., Singh, P., Sen, K., 2020. Selectivity of Th(IV) adsorption as compared to U (VI), La(III), Ce(III), Sm(III) and Gd(III) using mesoporous $Al_2O_3$. Separ. Sci. Technol. 56 (14), 2369–2384.

Kirby, H.W., Morss, L.R., 2006. Actinium. In: Morss, L.R., Edelstein, N.M., Fuger, J., Katz, J.J. (Eds.), The Chemistry of the Actinide and Transactinide Elements, vol. 1. Springer, The Netherlands.

Kratochwil, C., Bruchertseifer, F., Giesel, F.L., Weis, M., Verburg, F.A., Mottaghy, F., Kopka, K., Apostolidis, C., Haberkorn, U., Morgenstern, A., 2016. 225Ac-PSMA-617 for PSMA-targeted alpha-radiation therapy of metastatic castration-resistant prostate cancer. J. Nucl. Med. 57 (12), 1941–1944.

Lopes, C.F.F., Iha, K., Neves, E.A., Suárez-Iha, M.E.V., 2006. A comparison of carboxylate complexes of lanthanum (III): formate, acetate and propionate. J. Coord. Chem. 40 (1–2), 27–34.

Massart, D.L., 1971. Cation-Exchange Techniques in Radiochemistry, *Subcommittee on Radiochemistry*. National Academy of Sciences – National Research Council; U.S. Atomic Energy Commission pg 17.

Mcdevitt, M.R., Finn, R.D., Sgouros, G., Ma, D., Scheinberg, D.A., 1999. An Ac-225/Bi-213 generator system for therapeutic clinical applications: construction and operation. Appl. Radiat. Isot. 50, 895–904.

Mirzadeh, S., Mausner, L.F., Garland, M.A., 2003. Reactor-produced medical radionuclides. In: Vertes, A., Nagy, S., Klencsar, Z., Rosch, F. (Eds.), Radiochemistry and Radiopharmaceutical Chemistry in Life Sciences, vol. 4. Kluwer Academic Publishers, The Netherlands, p. 33.

Nagatsu, K., Suzuki, H., Fukada, M., Ito, T., Ichinose, J., Honda, Y., Minegishi, K., Higashi, T., Zhang, M.R., 2021. Cyclotron production of $^{225}$Ac from an electroplated $^{226}$Ra target. Eur. J. Nucl. Med. Mol. Imag. https://doi.org/10.1007/s00259-021-05460-7.

Nawrocki, J., Rigney, M.P., McCormick, A., Carr, P.W., 1993. Chemistry of zirconia and its use in chromatography. J. Chromatogr. A 657, 229–282.

Nawrocki, J., Dunlap, C., McCormick, A., Carr, P.W., 2004. Part I. Chromatography using ultra-stable metal oxide-based stationary phases for HPLC. J. Chromatogr. A 1028, 1–30.

Power, W.H., Kirby, H.W., McCluggage, W.C., Nelson, G.D., Payne, J.H.J., 1959. Separation of radium and barium by ion exchange elution. Anal. Chem. 31 (6), 1077–1079.

Radchenko, V., Morgenstern, A., Jalilian, A.R., Ramogida, C.F., Cutler, C., Duchemin, C., Hoehr, C., Haddad, F., Bruchertseifer, F., Gausemel, H., Yang, H., Osso, J.A., Washiyama, K., Czerwinski, K., Leufgen, K., Pruszynski, M., Valzdorf, O., Causey, P., Schaffer, P., Perron, R., Maxim, S., Wilbur, D.S., Stora, T., Li, Y., 2021. Production and supply of alpha-particle-emitting radionuclides for targeted alpha-therapy. J. Nucl. Med. 62 (11), 1495–1503.

Schulz, W.W., Koenst, J.W., Tallant, D.R., 1980. Applications of inorganic sorbents in actinide separations processes. In: Navratil, J.D., Schulz, W.W. (Eds.), Actinide Separations – ACS Symposium Series, vol. 117. ACS pg 17.

Severin, A.V., Vasiliev, A.N., Gopin, A.V., Enikeev, K.I., 2020. Sorption and diffusion behavior of actinium(III) ions in contact with hydroxyapatite as a transporter of medical radionuclides. Russian Chem. Bul. Int. Ed. 69 (12), 2286–2293.

Talip, Z., Eral, M., Hicsonmez, U., 2009. Adsorption of thorium from aqueous solutions by perlite. J. Environ. Radioact. 100 (2), 139–143.

Vasiliev, A.N., Zobnin, V.A., Pavlov, Y.S., Chudakov, V.M., 2020. Radiation stability of sorbents in medical $^{225}$Ac/$^{213}$Bi generators. Solvent Extr. Ion Exch. 39 (4), 353–372.